

Tomographic inversion and pre-stack depth migration of seismic profile KK-02 across the Krško plain

F. ACCAINO¹, L. CERNOBORI^{*1}, R. NICOLICH², G. ROSSI¹ and F. ZGUR¹

¹ OGS, Istituto Nazionale di Oceanografia e di Geofisica Sperimentale, Trieste, Italy

² University of Trieste, Italy

(Received: October 7, 2013; accepted: February 10, 2014)

ABSTRACT In this paper we discuss results of analyses made on two near-regional scale seismic profiles acquired in the area of Krško Nuclear Power Plant (NPP), in SE Slovenia. Geophysical and geological data were collected to improve the seismotectonic model that is aimed at the assessment of earthquake hazards. Accordingly, the identification of active faults was the main objective of seismic profiling. The program was completed in 2000 within the project “Geophysical Research in the surroundings of the Krško NPP”, supported by the EU under the PHARE Program, which finalized a grid of seismic prospecting completed by locally focalized high resolution profiling to define the position of faults extending very near the surface as accurately as possible. Two near regional lines, KK-02 and KK-03 are here analysed and discussed. Furthermore, the profile KK-02 was processed with a pre-stack depth migration after an accurate tomographic velocity inversion. The interpretation of the seismic sections so obtained points out two thrust faults developed during the Late Pontian-Pliocene, revealing the N-S tectonic compression. Continuity of these faults was studied from their nucleation inside the pre-Neogene basement to the near surface.

Key words: seismic survey, seismic tomography, Krško Nuclear Power Plant, Slovenia.

1. Introduction

Near-regional and high resolution seismic profiles were collected in 1999 in the frame of the project “Geophysical Research in the surroundings of the Krško Nuclear Power Plant (NPP)”, supported by the EU under the Phare Programme. The project was aimed at improving the understanding of the tectonic setting of the Krško basin (Fig. 1) and at indicating the presence of possibly active faults cutting through pre-Neogene basement and overlying Neogene and Quaternary sediments. It was designed with the aim of integrating and completing the previous gravity and seismic (single fold) data acquired for hydrocarbon prospecting in the area (Kaloper, 1984) and of high resolution profiles (Gosar, 1996, 1998, and references therein).

The main objectives were: i) to comprehensively image deep and near-surface structures of the basin; ii) to map faults, in particular those deforming Neogene and Quaternary strata, which

* Licio Cernobori passed away in 2000.

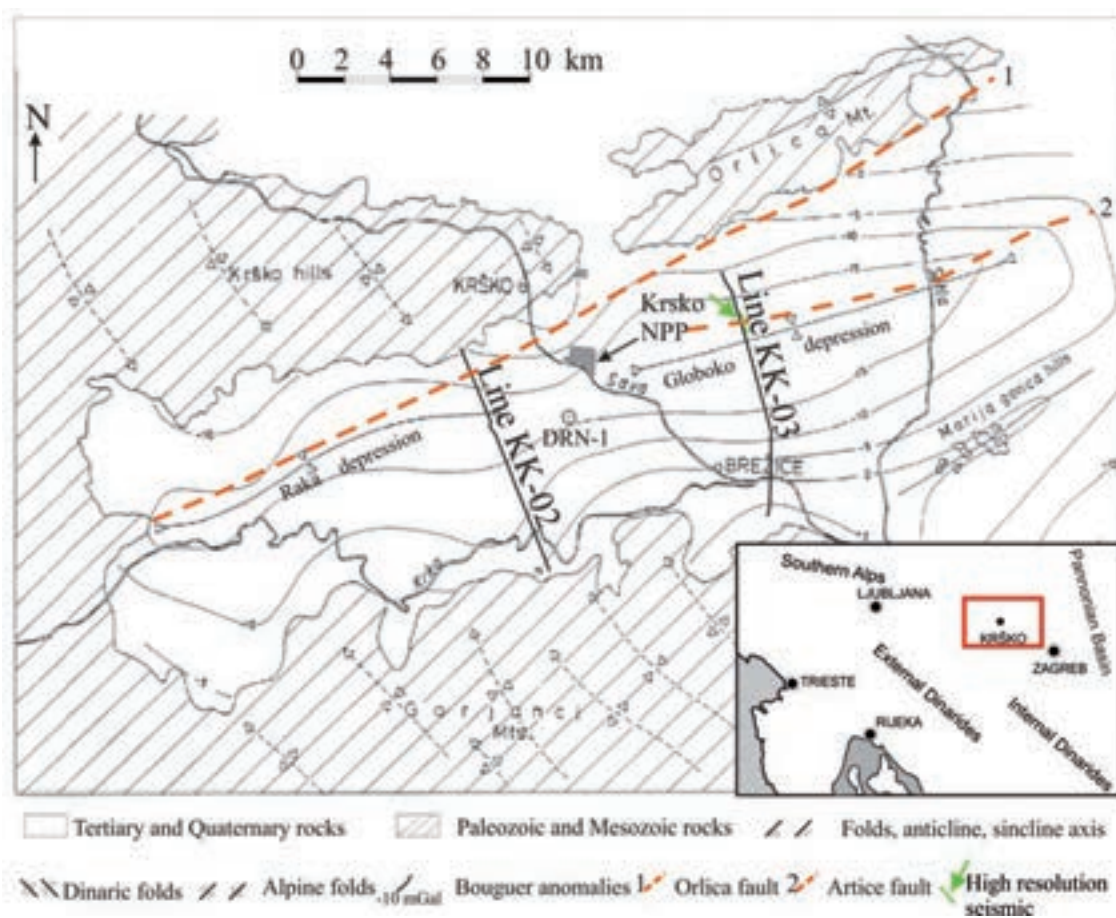


Fig. 1 - Simplified structural map of the Krško basin [compiled after the Basic Geological Map of SFRY 1:100,000, Pleničar *et al.* (1976) and Aničić and Juriša (1985)], and position map of the investigated seismic lines. Bouguer anomalies (contours interval: 5 mGal) from Gosar (2008); (1) Orlica fault from Placer (1998); (2) Artiče fault from Tomljenović and Csonos (2001).

accordingly could be attributed to on-going (recent) tectonic activity near the NPP (Persoglia *et al.*, 2000).

The seismic reflection method plays a key role when subsurface geologic structures have to be imaged in detail, and represents an important tool for the assessment of seismic hazard and construction of a reliable seismotectonic model. The surroundings of the Krško NPP were affected through time by numerous earthquakes, as the Brežice earthquake occurred in 1628 (with epicentral intensity VIII MCS), 1640 (IX MCS), 1917 ($M=5.7-6.2$) and the strong earthquake in 1880 (with epicentral intensity of VIII MCS), located between Krško and the city of Zagreb in Croatia (Herak *et al.*, 1996, 2009).

In this paper we discuss the results of analysis of two out of three reflection seismic lines acquired in the area, namely, KK-02 and KK-03 lines (Fig. 1), whose length is 10.3 km and 10.95 km, respectively. Acquisition parameters and geometries were defined on the basis of previous investigations and analysis of preliminary field tests and are reported in Table 1.

The two profiles are normal to the main axis of the Krško-Brežice plain, and, hence, are important for imaging not only its subsurface geometry, but also the basin controlling structures

Table 1 - Acquisition parameters for the seismic lines.

SPREAD	No. of traces	120
	Station interval	15 m
	Spread definition	1845 m, symmetrical split 4 trace gap (2 each side of source – 75 m) No gap in particular conditions
	Geophone array	Linear pattern (12 x 1 geophones of 12 Hz) Spacing 0.7 m; total length 7.7 m
	Source offset	37.5 m
SOURCE	Source type	Dynamite
	Source interval	60 m
	Charge size	Depending on the environment conditions 0,5 kg – normal conditions (open fields) 0,2 kg – near roads, houses, etc.
	Borehole depth	5-11 m (generally one metre below the water table)
COVERAGE	Nominal fold	15
INSTRUMENT.	Record length	4 s
	Sampling rate	1 ms
	High cut filter	350 Hz (slope 72 dB/oct)
	Low cut filter	16 Hz (slope 36 dB/oct)
	Notch filter	out
	Preamplifier gain	24 dB

and the most recent faults that cut across the youngest sedimentary sequences. The application of standard processing steps provided clear seismic images, namely the time-migrated and depth converted sections, used for the interpretation presented here. Also, very high resolution seismic data were collected in the area, to investigate the shallowest structures [for acquisition details, see Persoglia *et al.* (2000)]. In particular, we show one of them, added to profile KK-03 (see Fig. 1), in order to better image upward continuation of one of the regional tectonic lineaments evidenced on that line. Unfortunately, there are no similar profiles over line KK-02.

To correctly calibrate sedimentary layers geometry and their thickness, and to better image the character and throw of faults identified in the KK-02 profile, depth imaging techniques were adopted for this line. Pre-stack depth migration was computed by applying a depth velocity model derived from a tomographic inversion of the main reflectors recognized in the basin.

The results presented in this paper shed new light on the achievements previously gained (Gosar, 1998, 2008; Poljak and Gosar, 2000; Gosar and Božiček, 2006); moreover, they prove how seismic tomography can successfully support interpretation.

2. Geological setting of the Krško syncline

The term Krško basin, as used in this paper, refers to the Krško-Brežice plain, located in south-eastern Slovenia, filled up by sediments of Neogene and Quaternary age. The basin is surrounded by hilly terrains of the Krško hills and Orlica Mt. to the north, and the Gorjanci Mts. and Marija

Gorica hills to the south (Fig. 1). Structurally, it is a syncline of Late Miocene and Quaternary age located at the transition zone between the Internal Dinarides (to the east), the External Dinarides (to the west) and the Southern Alpine structures to the north (Poljak *et al.*, 2000). With respect to Neogene basin fill, this basin formed at the western rim of the Pannonian basin.

Palaeozoic rocks, documented by geological mapping (Pleničar *et al.*, 1976; Buser, 1978; Šikić *et al.*, 1978; Aničić and Juriša, 1985) on outcrops in the hilly region at the rims of the Krško plain are represented by clastic and carbonate Permian sediments [see also Haas *et al.* (2000) and references therein]. On geological maps of these authors, Mesozoic rocks are represented by Lower Triassic clastics, Anisian dolomites, Ladinian clastites and thick Upper Triassic dolomites. The successive Jurassic carbonates are overlain by Cretaceous sequences composed of carbonates and flysch units (Poljak and Gosar, 2000). Tertiary sediments are represented by Neogene carbonates and clastics (Table 2). The oldest Neogene rocks are sandy clays, gravels and conglomerates of Ottnangian age, deposited unconformably over the pre-Neogene basement. The presence of the Eggenburgian sediments cannot be excluded at least in the deepest parts of the basin (e.g., in the Globoko and Raka Krško sub-basins).

The Ottnangian clastics are overlain by Badenian limestones, followed discordantly by Sarmatian calcarenites and conglomerates, by Pannonian marls and Pontian sands and marls (Poljak *et al.*, 1996). The Pliocene-Quaternary cover is represented by sandy-gravel clastic sediments deposited in river terraces and by lateral lacustrine equivalents consisting of sands, silts and clays (Verbič *et al.*, 2004).

The values listed in Table 2 are maximal thickness compiled after Poljak *et al.* (1996). Additional data are available from the 1,252 m deep well DRN-1 (see Fig. 1 for well location), which penetrated through Neogene sediments and the Cretaceous basement (Kranjc *et al.*, 1990). Table 2 provides the correlation between stratigraphy and interpreted seismic horizons (P1 to C) as proposed by Gosar (1998)

Structurally, the investigated area exhibits heterogeneous pattern. Its structures express both “Dinaric” and “South-Alpine” deformational trends and their formation resulted from interaction and convergence of Adria with respect to the Dinaric-Pannonian domains. The Dinaric structural pattern, composed of NW-SE striking km-scale folds and faults of the Late Eocene age, is well expressed within Mesozoic rocks in the Krško Hills and in Gorjanci Mountains (Persoglia *et al.*, 2000).

Table 2 - Horizons marked on the seismic sections according to Gosar (1998) and controlled by the DRN-1 well stratigraphies (Kranjc *et al.*, 1990) with ages, approximate maximum thicknesses in the area and main lithologies.

Seismic Horizons	Age	Approx. max. Thickness (m)	Main lithologies	DRN-1 (m)
P1	Pliocene-Holocene	200	Sands, gravels, clays	50
P2	Upper Pontian	500	Marls	170
A	Lower Pontian	80	Sandy-marls	100
M	Pannonian	300	Marls	241
B	Sarmatian	100	Sandy-marls, Limestones	86
	Badenian	300		40
C	Ottnangian	300	Gravels, Sands	282
	Mesozoic		Marly-limestones,	T.D. 1252

After the Eocene compression, the area was affected by the onset of extensional tectonics, starting in Oligocene-Early Miocene, with the development of intra-mountain pull-apart basins associated with conjugate strike-slip faults (Ustaszewski *et al.*, 2008). The opening of extensional basins, where Ottnangian and Badenian sequences deposited, was a major event affecting the Dinarides edifice during the Early and Middle Miocene (Lučić *et al.*, 2001). In this context, the initial NE-SW transversal fault system, with dextral movement, was related to the extension of the Pannonian basin (Prelogović *et al.*, 1998; Tari and Pamić, 1998). The NW-SE striking right-lateral system of faults was generated by indenting of the Adria microplate against Europe, accompanied with eastward and south-eastward tectonic escape of the Eastern Alps towards the unconstrained Pannonian Basin (Ratsbacher *et al.*, 1991; Haas *et al.*, 2000; Ustaszewski *et al.*, 2008; Brückl *et al.*, 2010).

During Pannonian-Pontian times, a pronounced subsidence interested the Pannonian domain with the accumulation of thick post-rift sedimentary succession (Lučić *et al.*, 2001).

Due to the regional stress inversion of Late Miocene (Peresson and Decker, 1997) with new N-S compression, the eastward lateral extrusion in the Eastern Alps terminated and a new style of deformation commenced in Pliocene. This neotectonic phase, continuing to present times, had a strong impact on major structures, mostly reverse faults and km-scale folds composed of Neogene sequences (Prelogović *et al.*, 1998, Tomljenovic and Csontos, 2001). Strike-slip movements, with conjugate faults, with transtensions and transpression zones and counter-clockwise (CCW) rotations, driven by the CCW rotating Adria microplate are characterizing the study region in post-Pontian times, according to Marton *et al.* (2002) and Tomljenović *et al.* (2008).

Indication of on-going tectonic movements in the study area has been deduced from geodetic measurements that show gradual increase in annual vertical displacement rate in the range of 0-1 mm/yr of the Krško basin northern and southern rims towards its central part (Koler and Breznikar, 1999) that shows negative vertical displacement values reaching -0.5 mm/yr. On the other hand, recent seismic activity appears to be concentrated along the Orlica fault [traced in Fig. 1, after Placer (1998)] with focal mechanisms of some seismic events that suggest on-going strike-slip displacements as proposed by Poljak *et al.* (2000).

The Krško basin is composed of two sub-basins: the Raka sub-basin to the west, which is filled with up to 1600 m of Neogene and Pleistocene-Holocene sediments, and the Globoko sub-basin to the east, with up to 2050 m of similar sequences. A saddle separates the two sub-basins and may represent a Dinaric structure, as imaged in the seismic sections (Persoglia *et al.*, 2000).

3. Processing sequence and interpreted horizons

The main objective of seismic data processing was to obtain the most accurate and reliable image of the subsurface of the investigated area, to enhance coherent reflected signals whilst attenuating the noise, due to both the acquisition operations themselves (e.g., source-generated noise such as ground roll and air coupled waves) and environmental conditions (power cables induced noise, traffic, etc.). The adopted processing sequence was composed by steps presented in Table 3, each performed by extensive testing to derive the optimum parameters. It provided post-stack time-migrated depth-converted seismic sections of good quality, with several recognizable reflectors (Fig. 2 for the line KK-02; Fig. 3 for the line KK-03).

Table 3 - Processing sequences of the seismic data.

PROCESSING SEQUENCE
Quality control and trace editing
Amplitude recovery applying a gain function
Static correction
Surface consistent deconvolution
Common depth sorting (using for the binning the crooked line approach)
Velocity analysis
Normal move out corrections
Surface consistent residual static corrections
Velocity analysis
Mute of the refracted events
Stack
Time variant filtering
Time migration
Depth conversion

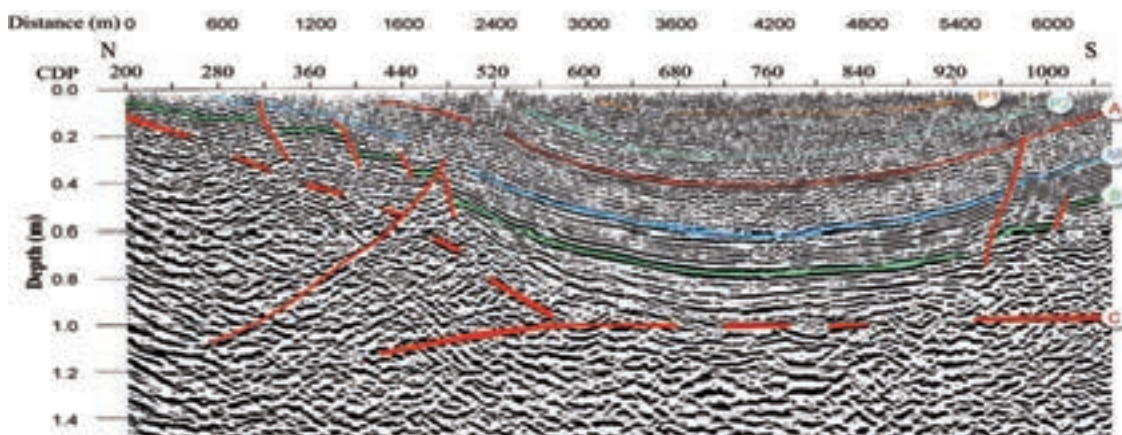


Fig. 2 - Part of the time-migrated and depth-converted section of the line KK-02 with interpreted horizons (after Accaino et al., 2003); the horizons C, B, M, A, P2, P1 are reported in Table 2.

3.1. Tomographic inversion of the line KK-02

Interpretation of seismic sections was based on the seismic horizons previously chosen by Gosar (1998) and by Persoglia et al. (2000) and tied with the DRN-1 well data (Table 2). We focus on the analysis of line KK-02 that shows two different fault systems at around 2.5 km and around 6.0 km from the northern beginning of the section in Fig. 2, respectively. The central part of the basin appears rather undisturbed.

The fault on the northern limb (at 2.5 km) is a thrust that appears to affect both the deep and

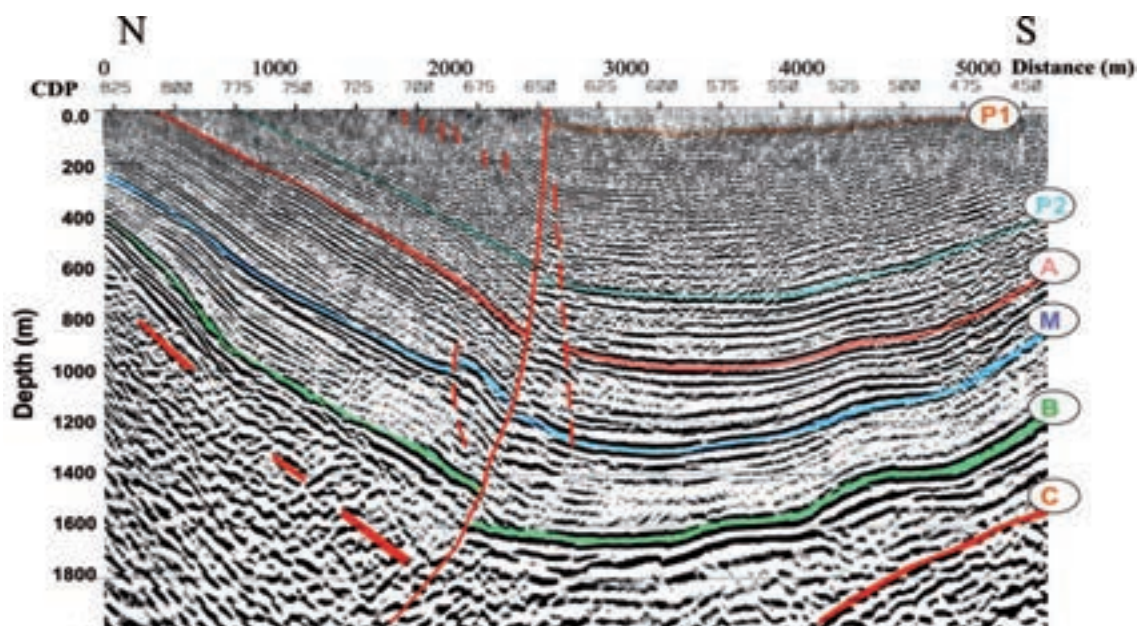


Fig. 3 - Interpretation of the time-migrated and depth-converted section KK-03 (after Accaino *et al.*, 2003); the horizons C, B, M, A, P2, P1 are reported in Table 2.

the shallow horizons. However, a clear interpretation of the relative displacements is not so easy to interpret on this section. To better understand the importance of these structures on the regional scale, we performed a tomographic inversion for a reliable velocity definition and the pre-stack depth migration of the data.

Seismic tomography is successfully applied to obtain a velocity field in depth that may be easily compared with well information, and can be an optimal input to perform a pre-stack depth migration, with the aim to obtain the correct geometry in depth of the tectonic structures (Vesnaver *et al.*, 2000; Yilmaz, 2001). The tomographic algorithm we used is discussed in detail in Böhm *et al.* (1999). The code inverts in sequence the velocity field and updates the reflector structure until their variations with respect to the previous step become sufficiently small [for details on the method, see, e.g., Vesnaver *et al.* (2000)]. The final result of the inversion has been improved by using the staggered grid method (Vesnaver and Böhm, 2000).

The first step of the inversion procedure is the picking of the horizons in the pre-stack domain. It requires particular attention for interpreting correctly primary reflections. In fact, the pre-stack data are characterised by several uncertainties, such as:

- lower signal/noise ratio in the pre-stack domain in respect to the full coverage stacked or migrated sections;
- interference of multiples, diffractions and anomalous events with a different Move Out trend;
- multi-pathing of signals due to structural complexities;
- out-of-plane arrivals;
- no-regular acquisition geometry and low coverage.

To avoid some of the mentioned problems and to aid the picking, static corrections and residual static corrections were applied in advance to improve the “continuity” of the reflections and better identify the travel times in the shot gathers.

Interpretation of the stacked section is needed before picking in the pre-stack domain to have an initial depth model. This was obtained by converting the stack velocities into interval velocities and by depth converting the line-drawing obtained from the interpretation of Gosar (1998), Persoglia *et al.* (2000), Accaino *et al.* (2003). The resulting six main reflectors are shown in Fig. 2 and listed in Table 2 (Accaino *et al.*, 2003). Only locally some reflectors are recognizable in the stacked section below reflector C within the pre-Neogene basement. The reflector C itself was sometimes hard to recognise and pick.

We utilised this rough model to calculate, through a ray tracing, using the acquisition geometry of the line, the predicted travel-times of the reflections in the pre-stack domain. In this way, we had an initial guide for the picking, of particular help in case of the shallowest interfaces and in presence of on-lapping sequences.

The initial travel times picking was refined iteratively at each tomographic inversion step. Namely, the procedure consisted in: i) inverting the travel times, ii) estimating a depth model, (iii) predicting new travel times, and iv) revise the picked travel times.

Fig. 4 shows a common shot gather in the central area of the line where the six reflectors (P1 to C in Table 2) are picked. An example of predicted travel times (white dots) of one of the reflectors is also shown. The agreement between the predicted and original picking, confirms the validity of this procedure.

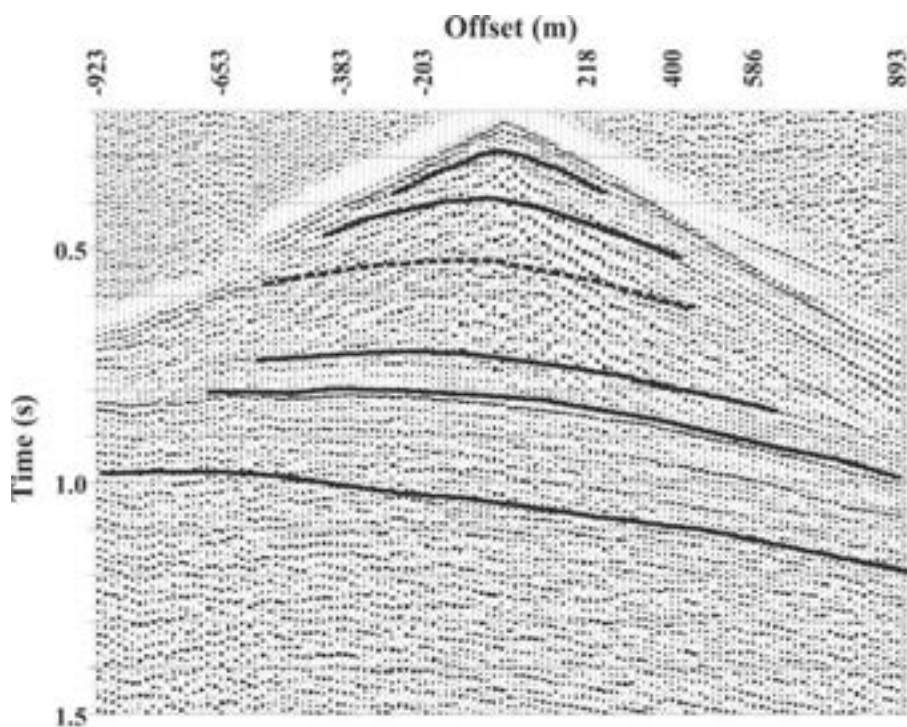


Fig. 4 - Example of picking in the shot domain. White squares in the third reflector correspond to the reflection times predicted by the tomographic model.

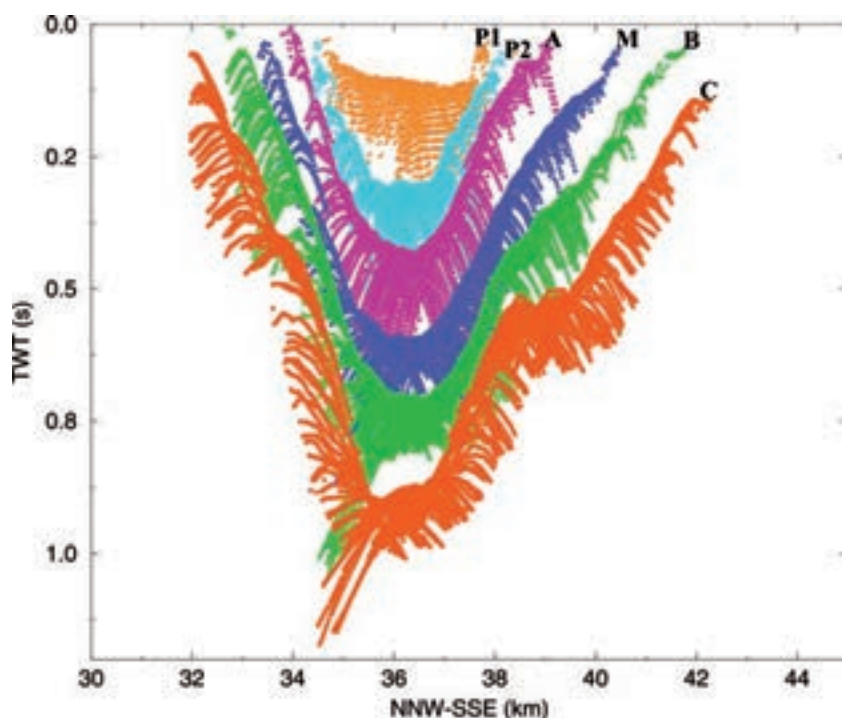


Fig. 5 - Picked events in the shot domain used for the tomographic inversion of the line KK-02.

However, the inversion of the line KK-02 is characterised by several difficulties, related to complex geometrical stratigraphic structures. To better constrain the lateral velocity variations, we used velocity pixels 150 m wide. The geometry of reflections was improved by considering a large number of picks to build each interface (one point every 100 m) and by carrying on picking on all the shots of the seismic line. Fig. 5 shows all picked travel times utilised for the inversion: the move-out at greater offsets is evident.

The procedure for the inversion can be defined as a layer stripping approach and can be summarised in four steps:

- 1) picking of the travel times of the first interface (bottom of the first layer);
- 2) inversion of the velocity of the first layer;
- 3) estimate of the new position and geometry of the interface;
- 4) ray tracing with the improved depth velocity model of the first layer;
- 5) refinement of the picking and new inversion.

The procedure is iterated until the final achievement of satisfactory results (minimal difference between predicted and picked travel times), and the steps 1) to 5) were applied to the next layer. At every new layer the new picking is added to the previous one. In this way we have inverted all the layers until the last one and refined by tomographic modelling also the velocities of all the overlying layers, previously inverted.

The final velocity model of the line KK-02 is shown in Fig. 6 and was used to compute the pre-stack depth migration, obtaining a depth imaging across the Krško syncline.

Table 4 summarizes the main results: the average interval velocities of each layer, as well

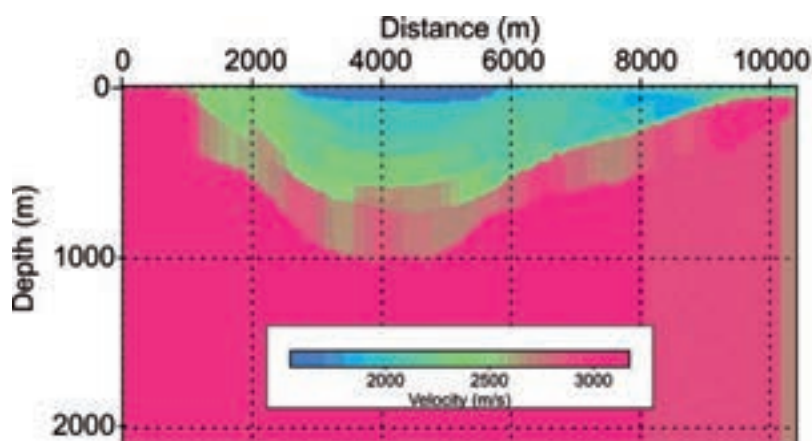


Fig. 6 - Tomographic velocity field of the line KK-02.

Table 4 - Interval velocities and maximum thicknesses of the litho-stratigraphic intervals resulting from tomographic inversion and pre-stack migration.

Int.	Tomographic interval velocity (m/s)	Tomographic max. thickness (m)
P1	1600-1650	115
P2	1900-1950	185
A	2000-2200	115
M	2300-2400	220
B	2500-2600	130
C	2700-2850	245
	2900-3300	

as the maximum thickness estimated with our tomographic inversion. The depth of the pre-Neogene basement is comparable with the depth measured in the well DRN-1, while the layer thickness in some cases is different, as for the shallowest reflectors that result thicker in the tomographic model. We recall, however, that DRN-1 was drilled more than 3 km off the line, at the center of the saddle separating the Raka and Globoko sub-basins, which can partially explain observed differences. The velocity is not homogeneously distributed: as we can see on Fig. 6, in the layer between horizons C and B higher velocities are present in the central part of the basin and a further high velocity anomaly is present at about 6500 m from the beginning of the section.

In addition, we tentatively identified some locally reflective markers within the Mesozoic sequences (i.e., below horizon C). The inversion gave a velocity of 2900-3000 m/s at the beginning and at the end of the profile for these intervals, while under the centre of the basin we obtained a velocity of 3100-3300 m/s. This information is important to complete the depth velocity model, which is the input for the depth-migration procedure, avoiding noise of over-migrated deeper events, underlying the interpreted horizons.

3.2. Pre-stack depth migration of line KK-02-99 and interpretation of structures

The velocity field obtained by seismic tomography was used to perform the pre-stack depth migration. The same processing sequence used to obtain the stack section (Table 3) was applied before the migration to improve the S/N ratio of pre-stack seismic data.

The velocity field was verified, upgraded and improved step-by-step by iteratively applying the pre-stack depth migration using the staggered grids method (Vesnaver and Böhm, 2000). In Fig. 7, the smoothed velocity field is superimposed to the final pre-stack depth migration. The good agreement of the seismic facies with the velocities distribution, indicates the reliability of the final result.

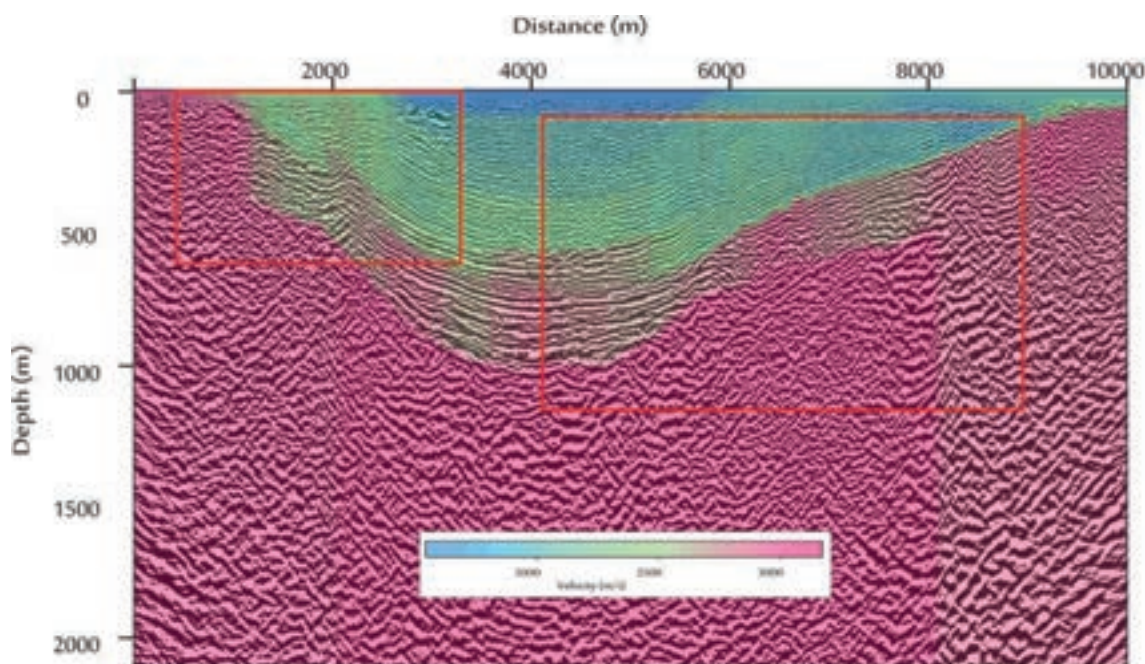


Fig. 7 - Pre-stack depth migrated section of line KK-02 with superimposed the smoothed tomographic velocity field. The red boxes indicate the zooms in Figs. 9 and 10, respectively.

The two red boxes in Fig. 7 point to the position of the blow-ups showed in Figs. 8 and 9. They show the most important tectonic structures with a good resolution in the depth domain and give a significant aid to the geological interpretation.

In Fig. 10 the pre-stack depth interpreted section of the line KK-02 is shown with six main reflectors marked together with interpreted fault traces. At about 2.4 km from the northern end of the line a north-dipping reverse fault was interpreted displacing all interpreted horizons. At about 6 km from the north, a normal fault was interpreted, which does not reach the surface. This fault displaces horizons B and C with a normal sense of slip, while the shallowest horizons (M-P1) seem to be only slightly affected. Other minor normal growing faults are present in the central part and southern limb of the syncline, while north-verging reverse faults appear to cut across the pre-Neogene basement and Ottnangian deposits.

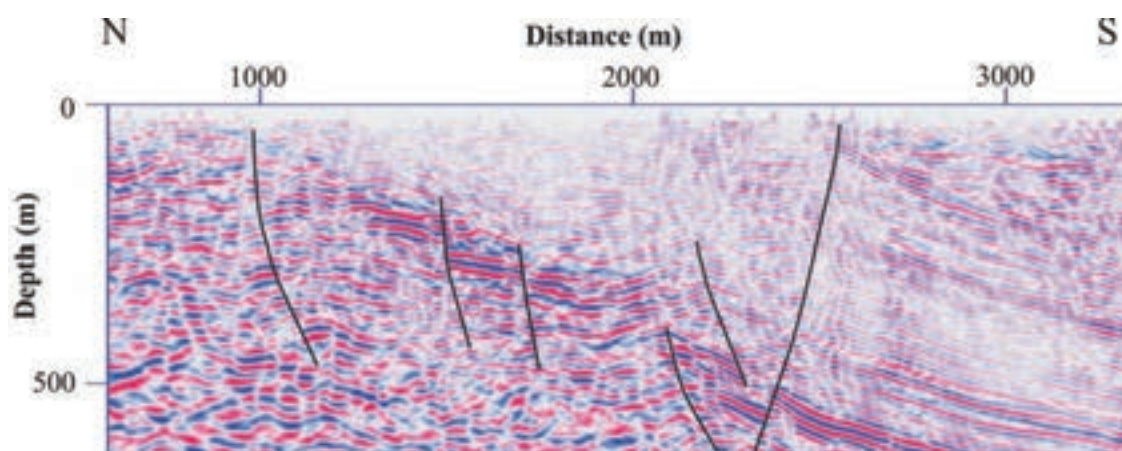


Fig. 8 - Zoom of the line KK-02: the red box on the left of the Fig. 8. Vertical exaggeration 1:1.5.

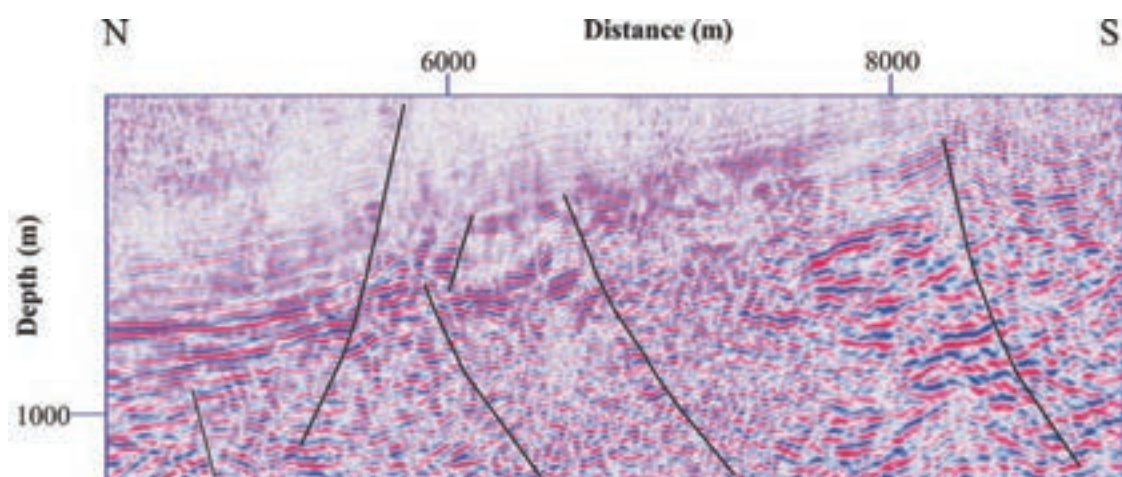


Fig. 9 - Zoom of the line KK-02: the red box on the right of the Fig. 8. Vertical exaggeration 1:1.5

4. Discussion and conclusions

The depth converted seismic sections of the two investigated lines (Figs. 2 and 3) provide an optimum seismic image of the Neogene and Quaternary layers in the studied part of the Krško basin. The major depositional sequence boundaries and fault traces at depth and near the surface have been interpreted, yielding new information about subsurface structures of this part of the Krško syncline. The results confirm about the right choice of acquisition parameters and processing sequence.

Gravity modeling of the basin was completed by Gosar and Božiček (2006) and by Gosar (2008) in order to extend the interpretation beyond the seismic profiles. They proposed that the present day structure of the basin is an asymmetric syncline with a pronounced step on

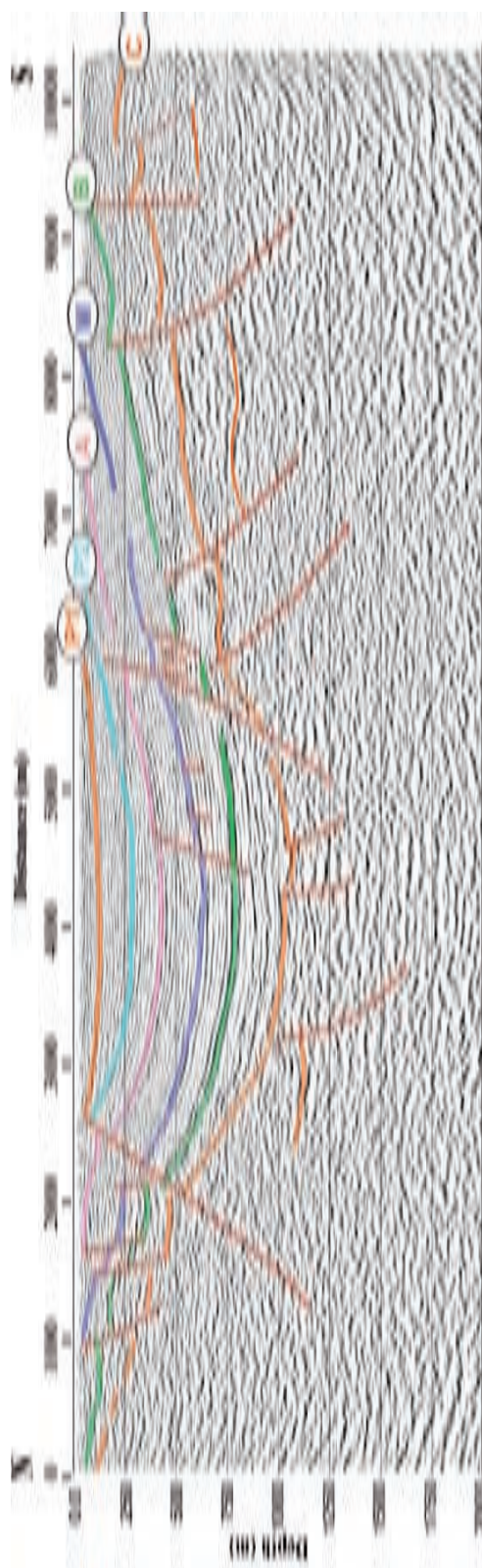


Fig. 10 - Interpretation of the pre-stack depth migrated section KK-02.

the northern side and uniform thinning of the Quaternary strata towards the south. The higher resolution of our seismic images points out the importance of the south-verging thrusts, which are in correlation with the **Artiče fault mapped along the southern slope of Krško Hills, and the northern limb of the Krško syncline** (Poljak and Gosar, 2000).

Tomographic inversion and the consequent pre-stack depth-migration applied to the line KK-02 improve imaging of tectonic structures, not everywhere evident in the post-stack time migrated and depth-converted section. **The top of the pre-Neogene basement is not evident in all places in this line because of poor impedance contrasts between sediment successions and because of severe tectonization. The Lower Miocene (Ottangian) sequences are transgressively deposited over the pre-Neogene basement as shown by on-lapping of seismic horizons** (see Fig. 10 and the left part of the zoom in Fig. 8). The thickness of this unit varies in our interpretation from 20 to 50 m in the northern part and up to about 300 m in the southern part of the section where the S/N ratio is poor and the character of reflection is lost. In the central part of the section, this unit is less affected by tectonic deformation and its thickness ranges from 100 to 200 m.

We have indicated, on the southern limb of the section in Fig. 10 (and in the zoom of Fig. 9), the presence of north-verging reverse faults in pre-Neogene basement that propagated into Ottangian sequences.

In the central part and in the southern limb of the Krško syncline the Neogene reflectors lie nearly parallel to the northward dipping pre-Neogene substratum, with indications of few normal faults (Fig. 10, sector at distances from 4500 to 6200 m). In our interpretation, this set of north-dipping normal faults with small vertical offset, displaces Badenian and Pannonian sequences. One of these faults (at about 6000 m distance) is interpreted to cross-cut the basin from the pre-Neogene basement up to Lower Pontian strata.

The dominant structures indicate a N-S compression, which controlled the post-depositional folding and faulting that appear to start in Late Pontian. The strongly dissected anticline structure of the Krško Hills slope is limited in the pre-stack migrated depth section by a reverse fault (Fig. 10). The anticline is also apparently displaced by a set of normal faults outlined in the shallow part of the sections in Figs. 8 and 10. **A better definition of these fractures is not possible with our seismic imaging, for the resolution loss towards the surface as well as into the pre-Neogene basement.** They should correspond to the south-westwards continuation of the Orlica fault zone. We refer to the supposed Orlica fault trace and orientation in Fig. 1 (after Placer, 1998), considered a presently active strike-slip fault (Poljak *et al.*, 2000), but we are not able to detect its exact position and nature.

Within the resolution of seismic images, near surface reflectors corresponding to Quaternary strata appear not disturbed in the centre of the syncline with nearly sub-horizontal layering thinning mostly southwards with transgressions and onlaps (at distances from 3000 to 5500 m in Fig. 10). The Quaternary filling of the structural depression took place in the front of the south-verging thrust and may confirm the decrease of the tectonic activity in the Quaternary. The above described structural setting and evolution of the Krško basin can be confirmed by the profile KK-03, which crosses the eastern sector of the syncline. The N-S compression is once more evidenced in this line (Fig. 3) with a reverse fault, appearing to reach very shallow depths at the northern limb of the Globoko sub-basin. It displaces the pre-Neogene basement as well as the Neogene sequences. Near the surface, the fault throw apparently decreases, leaving only the warping of recent deposits. This south-verging reverse fault can be associated with

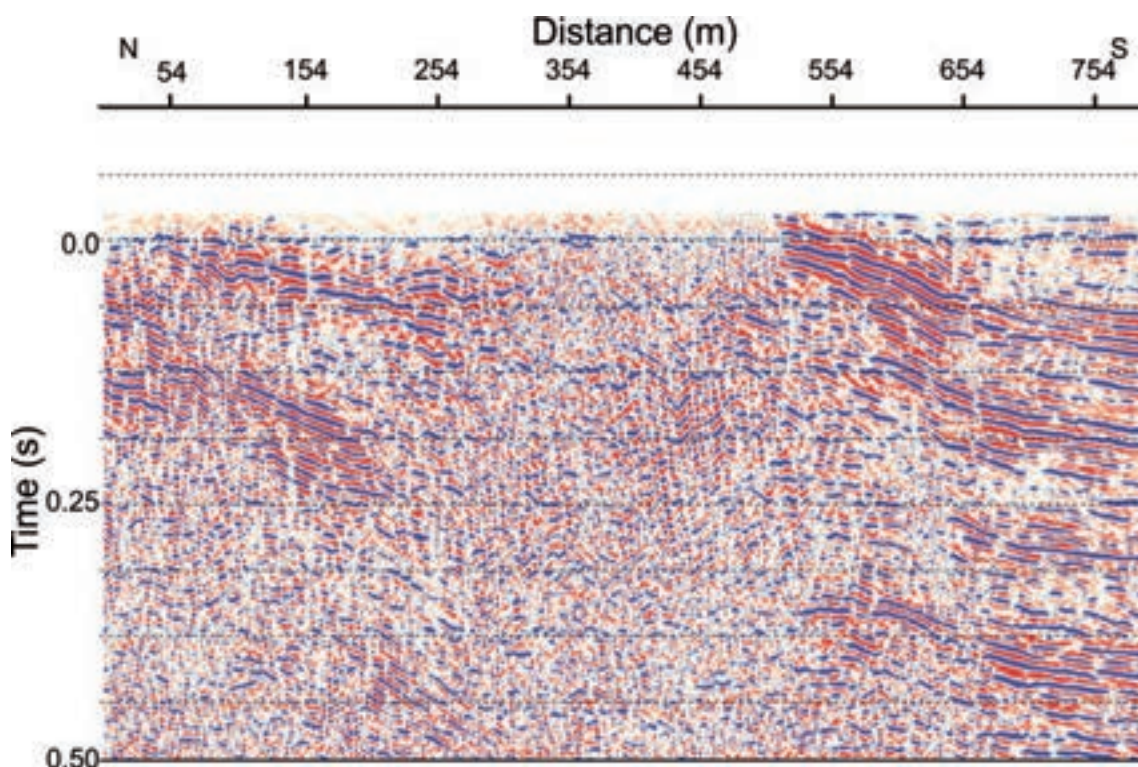


Fig. 11 - Part of the stacked section of a high resolution seismic line highlighting the shallow tectonic structures along the profile KK-03 [modified after Persoglia *et al.* (2000), location indicated in Fig. 1].

the Artiće fault zone documented in outcrops that probably merge westwards into the southern thrust front of the Krško Hills and Orlica system and continues eastwards from Krško syncline into Konjščina syncline in Croatia, in conformity with the interpretation of seismic profiles published by Tomljenović and Csontos (2001).

The high resolution data (Fig. 11) confirms the warping of the shallow deposits at the northern rim. It shows also the well resolved and undisturbed Quaternary filling of the depression at the center of the line, mostly thinning to the south and to the north, similarly to what observed on the line KK-02. Alternation of dominantly compressive versus dominantly extensive periods followed by strike-slip displacements (NW-SE and NE-SW directed faults) is characterizing the Neogene evolution of the area (Prelogović *et al.*, 1998; Tomljenović and Csontos, 2001). The present reactivation of sinistral and dextral strike-slip faults, and an initial warping and folding of shallow deposits, accompanied by the on-going movements from geodetic measurements, may be of importance for seismotectonic modeling of the Krško-NPP area.

Acknowledgements. The authors would like to thank Anna Del Ben and an anonymous reviewer for the careful reading, constructive discussions and the valuable comments of the results presented in this paper. The research was done within the EU-project PHARE 98-0286.00. The authors are grateful to all the project partners, which variously contributed to it.

REFERENCES

- Accaino F., Gosar A., Millhan K., Nicolich R., Poljak R., Rossi G. and Zgur F.; 2003: *Regional and high-resolution seismic reflection investigations in the Krško Basin (SE-Slovenija)*. Ann. Univ. Sci. Bp. Rolando Eötvös Nomin., Sect. Geol., **35**, 116-117.
- Aničić B. and Juriša K.; 1985: *Basic geological map of SFRY 1:100 000 sheet Rogatec*. Federal Geological Survey, Beograd.
- Böhm G., Rossi G. and Vesnaver A.; 1999: *Minimum-time ray-tracing for 3-D irregular grids*. J. of Seismic Exploration, **8**, 117-131.
- Brückl E., Behm M., Decker K., Grad M., Guterch A., Keller G.R. and Thybio H.; 2010: *Crustal structure and active tectonics in the Eastern Alps*. Tectonics, **29**, 1-17, doi: 10.1029/2009TC002491.
- Buser S.; 1978: *Basic geological map of SFRY 1:100 000, sheet Celje*. Federal Geological Survey, Beograd.
- Gosar A.; 1996: *Seismic reflection method in structural investigations for assessment of earthquake hazard in the Krško basin*. Ph.D. thesis, Univ. of Ljubljana, Ljubljana, Slovenia, in Slovenian, with English abstract.
- Gosar A.; 1998: *Seismic-reflection surveys of the Krško basin structure: Implications for earthquake hazard at the Krško nuclear power plant, SE Slovenia*. J. of Applied Geophysics, **39**, 131-153.
- Gosar A.; 2008: *Gravity modelling along seismic reflection profiles in the Krško basin (SE Slovenia)*. Geologia Carpathica, **59**, 147-158.
- Gosar A. and Božiček B.; 2006: *Structural maps of seismic horizons in the Krško basin*. RMZ - Materials and Geoenvironment, **53**, 339-352.
- Haas J., Mioč P., Pamić J., Tomljenović B., Árkai P., Bérczi-Makk A., Koroknai B., Kovács S. and Felgenhauer E.R.; 2000: *Complex structural pattern of the Alpine-Dinaridic-Pannonian triple junction*. Int. J. Earth Sci., **89**, 377-389.
- Herak M., Herak D. and Markušić S.; 1996: *Revision of the earthquake catalogue and seismicity of Croatia (1908-1992)*. Terra Nova, **8**, 86-94.
- Herak D., Herak M. and Tomljenović B.; 2009: *Seismicity and earthquake focal mechanism in North-Western Croatia*. Tectonophysics, **465**, 212-220.
- Kaloper D.; 1984: *Krsko polje-Brezice, analogna obrada*. Technical report, Geofizika Zagreb.
- Koler B. and Breznikar A.; 1999: *Določitev vertikalnih premikov na območju Krškega in Krške kotline*. 5. strok. srečanje Slov. zdruz. geod. geof., Ljubljana 15.12.1999, Zbor. predavanja II del, 31-49, Ljubljana.
- Kranjc S., Božović M. and Matoz T.; 1990: *Končno poročilo o geoloških raziskavah na Krškem polju za potrebe podzemnega skladiščenja plina, Vrtina DRN-1/89*. Geološki zavod Slovenije, Ljubljana (unpublished report).
- Lučić D., Saftić B., Krimanić K., Prelogović E., Britvić E., Mesić I. and Tadej J.; 2001: *The Neogene evolution and hydrocarbon potential of the Pannonian Basin in Croatia*. Marine and Petroleum Geology, **18**, 133-147.
- Marton E., Pavelić D., Tomljenović B., Avanić R., Pamić J. and Marton P.; 2002: *In the wake of a counterclockwise rotating Adriatic microplate: Neogene paleomagnetic results from Northern Croatia*. Int. Journ. of Earth Sciences, **91**, 514-523.
- Peresson H. and Dekker K.; 1997: *Far-field effects of Late Miocene subduction in the Eastern Carpathians: E-W compression and inversion of structures in the Alpine-Carpathian- Pannonian region*. Tectonics, **16**, 38-56.
- Persoglia S., Cernobori L., Gosar A., Millhan K., Nicolich R., Nieto D., Poljak M., Terreros M., Vesnaver A. and Wardell N.; 2000: *Geophysical research in the surroundings of the Krško NPP - Final Report*. European Commission – DG IA – PHARE, 68 pp. (unpublished report).
- Placer L.; 1998: *Contribution to the macro-tectonic subdivision of the border region between Southern Alps and External Dinarides*. Geologija, **41**, 223-255.
- Pleničar M., Premru U. and Herak M., 1976. *Basic geological map of SFRY 1:100000, sheet Novo Mesto*. Federal Geological Survey, Beograd.
- Poljak M. and Gosar A.; 2000: *Strukturna zgradba Krške kotline po podatkih geofizikalnih raziskav v letih 1994-2000*. Geoloski zbornik, **16**, 79-82.
- Poljak M., Verbič T., Gosar A., Živčič M. and Ribičič M.; 1996: *Neotektonske raziskave na območju JE Krško, Zaključno poročilo*. Technical report, Geological Survey of Slovenia, Ljubljana.
- Poljak M., Živčič M. and Zupancic P.; 2000: *The seismotectonic characteristics of Slovenia*. Pure Appl. Geophys. **157**, 37-55.

- Prelogović E., Saftić B., Kuk V., Velić J., Dragas M. and Lučić D.; 1998: *Tectonic activity in the Croatian part of the Pannonian basin*. *Tectonophysics*, **297**, 283-293.
- Šikić K., Basch O. and Šimunic A.; 1978: *Basic geological map of SFRY 1:100 000, sheet Zagreb*. Federal Geological Survey Beograd.
- Ratshbacher L., Frisch W., Linzer H.G. and Merle O.; 1991: *Lateral extrusion in the Eastern Alps, part 2: structural analysis*. *Tectonics*, **10**, 257-271
- Tari V. and Pamić J.; 1998: *Geodynamic evolution of the northern Dinarides and the southern part of the Pannonian Basin*. *Tectonophysics*, **297**, 269-281.
- Tomljenović B. and Csontos L.; 2001: *Neogene-Quaternary structures in the border zone between Alps, Dinarides and Pannonian Basin (Hrvatsko zagorje and Karlovac Basins, Croatia)*. *Int. J. Earth Sciences (Geol. Rundsch.)*, **90**, 560-578.
- Tomljenović B., Csontos L., Márton E. and Márton P.; 2008: *Tectonic evolution of the northwestern Internal Dinarides as constrained by structures and rotation of Medvednica Mountains, North Croatia*. In: Siegesmund S., Fügenschuh B and Frotzheim N. (eds), *Tectonic Aspects of the Alpine-Carpathian-Dinaride System*. Geological Society, London, Special Publications, 298, pp. 145-167.
- Ustaszewski K., Schmid S.M., Fügenschuh B., Tischler M., Kissling E. and Spakmann W.; 2008: *A map-view restoration of the Alpine-Dinaridic system for the Early Miocene*. *Swiss J. Geosci.*, **Supplement 1**, S273-S294, doi: 10.1007/900015-008-1288-7.
- Verbić T., Rižnar, Poljak M., Demšar, M. and Toman M.; 2004: *Quaternary Sediments of the Krško Basin*. In: *Proceedings of the Second Croatian Geological Congress*, Dubrovnik, pp. 451-457.
- Vesnaver A. and Böhm G.; 2000: *Staggered or adapted grids for seismic tomography?* *The Leading Edge*, **9**, 944-950.
- Vesnaver A., Böhm G., Madrussani G., Rossi G. and Granser H.; 2000: *Depth imaging and velocity calibration by 3D adaptive tomography*. *First Break*, **18**, 303-312.
- Yilmaz Öz; 2001: *Seismic data analysis: processing, inversion, and interpretation of seismic data*. *Investigations in Geophysics*, no. 10, Society of Exploration Geophysicists, Tulsa, OK, USA.

Corresponding author: Flavio Accaino
OGS - Istituto Nazionale di Oceanografia e di Geofisica Sperimentale
Borgo Grotta Gigante 42c, 34010 Sgonico (TS), Italy
Phone: +39 040 2140467; fax: +39 040 327307; e-mail: faccaino@inogs.it

